Bioelectrochemistry 77 (2010) 100–105

Contents lists available at ScienceDirect

Bioelectrochemistry

journal homepage: www.elsevier.com/locate/bioelechem

Electrochemical determination of calf thymus DNA on Zr(IV) immobilized on gold–mercaptopropionic-acid self-assembled monolayer

Reza Karimi Shervedani *, Sima Pourbeyram

Department of Chemistry, University of Isfahan, Isfahan 81746-73441, Islamic Republic of Iran

ARTICLE INFO

Article history:
Received 21 February 2009
Received in revised form 3 July 2009
Accepted 3 July 2009
Available online 15 July 2009

Keywords:
Zirconium
Calf thymus DNA
Electrochemical impedance spectroscopy
Self-assembled monolayers
DNA sensor

ABSTRACT

An electrochemical biosensor, constructed by immobilization of Zr(IV) on the topside of gold–mercaptopropionic acid self-assembled monolayer (Au–MPA–Zr SAM), is developed for the sensitive quantification of calf thymus DNA (ct-DNA). The sensor is based on ionic adsorption of ct-DNA from its phosphate backbone onto the Au–MPA–Zr(IV) SAM electrode. Preparation, characterization, and application of the sensor for determination of ct-DNA are described by cyclic voltammetry (CV), electrochemical impedance spectroscopy (EIS), and Osteryoung square wave voltammetry (OSWV) in the presence of an appropriate redox reaction probe. Parameters influencing the method have been tested. A linear range calibration curve from 1.0×10^{-4} to 5.0×10^{-7} g mL^{-1} ct-DNA with a detection limit of 9.5×10^{-8} g mL^{-1} and mean of relative standard deviations (R.S.D) of 2.5% for $n=4$ at each point was observed in the best conditions by EIS. Regeneration of the surface was carried out successfully by 5 min sonication in 0.1 M KOH solution and then 1 min incubation in 1.0×10^{-3} M Zr(IV) with a good reproducibility, R.S.D = 1.5% for $n=4$ as detected by EIS. The long-term storage stability of the electrode was also studied.

1. Introduction

Quantitative detection of nucleic acids, as a kind of the most important substances involved in vital movements, is of great significance in routine investigations like gene identification, molecular biology, biotechnology, medical diagnosis, forensic science, and environmental protection. Thus, several methods have been developed based on spectroscopy [1], chemiluminescence [2], resonance light scattering [3], fluorescence [4], phosphorescence [5], chromatography [6] and electrochemical [7] techniques for sensing of DNA.

Recent progresses in electrochemistry of nucleic acids have made the electrochemical detection platform a powerful alternative to the optical detection principles used in most of the current commercially available gene analyzers [7]. Electrochemical detection assays benefit of some advantages like being simple, reliable, cheap, sensitive, and selective for genetic detection [8]. Besides, the instrumentation is lightweight, compact, can easily be taken into the field and readily be automated [9]. The possibility of direct electrochemical detection of DNA was initially proposed by Palecek [10] who recognized the capability of both DNA and RNA to yield reduction and oxidation signals on the mercury electrode. Later, several solid-state electrodes, such as carbon paste electrodes [11], were employed to trace the electrochemical behavior of nucleic acids. However, the reported overpotentials of DNA bases at these electrodes have been usually large. For example, the anodic peak obtained at a carbon paste electrode, coming from the oxidation of guanine bases, is located at ca. 1.03 V [12], besides, voltammetric peaks are poorly developed. Thus, electrochemical methods applied for DNA analysis have generally shown a low sensitivity, except where highly sensitive techniques, such as electrocatalytic oxidation methods of the DNA bases, have been employed [13–15]. The DNA biosensors that rely on the immobilization of a single-strand DNA (ss-DNA) probe onto a surface are alternative methods for determination of DNA concentration via recognition complementary sequence (target DNA) by hybridization. However, quantitative determination methods developed based on hybridization process suffer from some limitations like (i) the need of immobilization of probe DNA on the electrode surface and (ii) the hybridization with complementary strand, which is time consuming. Therefore, these types of DNA biosensors are more suitable for DNA investigations such as sequence, damage or mismatch detection of target DNA, instead of concentration determination. In addition, this technique is incompatible for determination of unknown, long, native or double strand DNA (ds-DNA) concentration. On the other hand, industrial biopharmaceutical laboratories, as an example, need sensitive, simple and rapid DNA concentration determination methods [16]. Therefore, it remains a central problem to find an appropriate chemically modified electrode for simple and fast determination of DNA concentration in solution.

Chemical modification of the electrode surface is of great importance in electrochemistry including a wide spectrum of promising applications. In particular, thin films and self-assembled monolayers (SAMs) have been used in electroanalytical chemistry for

* Corresponding author. Tel.: +98 311 7932715.
E-mail address: rkarimi@sci.ui.ac.ir (R.K. Shervedani).

1567-5394/$ – see front matter © 2009 Elsevier B.V. All rights reserved.
doi:10.1016/j.bioelechem.2009.07.001

modification of the electrodes to develop sensors [17,18] and biosensors [19,20]. Further modification of the SAMs may allow fabrication of highly sensitive and more sophisticated sensors and biosensors for trace analysis.

Recent studies have shown that incorporation of metals or metal-binding units with desired electrical, magnetic, optical, and catalytic properties, or molecular recognition abilities into the gold–thiol SAMs can be used for the development and fabrication of sensors. Among the metal cation binding glues, Zr(IV) ion has found important applications due to its interesting properties [21]. For example, strong ionic and coordinative interactions between Zr(IV) ion and phosphate groups confirmed by several surface sensitive techniques [22,23], formation of functionalized thin films through Zr(IV) ions coordinated to phosphate groups [24], and immobilization of polycyclic aromatic hydrocarbons using Zr(IV) via phosphate–carbonate [25] on the solid surfaces have been reported by some authors. Similar studies have demonstrated applications of Zr(IV) for immobilization of biological molecules. For example, immobilization of laccase via enzyme carboxylate terminal groups [26], adsorption of DNA via phosphate groups [27,28], and immobilization of ds-DNA via its terminal phosphate [29] onto the solid surfaces have been cited.

Alternatively, these behaviors may allow immobilization of Zr(IV) on gold–thiol carboxylated electrode surface (e.g. on gold–mercapto-propionic) to prepare Au–MPA–Zr(IV) SAM for accumulation, and then, quantitative determination of DNA. Despite these interesting behaviors, no previous report has been published on Au–thiol–Zr(IV) SAM modified electrodes for DNA detection. In a recent report [30], we demonstrated that Au–MPA–Zr(IV) SAM electrode could be used for determination of phosphate, based on the strong ionic coordinative interactions between Zr(IV) and PO_4^{3-} groups.

In the present work, preparation, electrochemical characterization, and application of a new biosensor based on Zr(IV) immobilized on Au–MPA–Zr(IV) SAM electrode for determination of calf thymus DNA (ct-DNA) using cyclic voltammetry (CV), electrochemical impedance spectroscopy (EIS), and Osteryoung square wave voltammetry (OSWV) are intended. The experimental data will be presented and discussed from which the merits of the sensor will be introduced.

2. Experimental

2.1. Reagents

Calf thymus DNA (ct-DNA) from sigma, Zirconium chloride ($ZrCl_4$), 3-mercaptopropionic acid (MPA) and other chemicals were of analytical grade purchased from commercial sources (Merck or Sigma) and used as supplied. All solutions were prepared with purified water (18 MΩ cm, Millipore-MilliQ, Millipore Inć. France). Acetate buffer saline (ABS) solution was prepared by 0.1 M acetic acid solution in 1.0×10^{-2} M NaCl, and the pH was adjusted with NaOH or HCl solutions. Dilute solutions of ct-DNA were prepared immediately before use from a stock solution 1.0×10^{-4} g mL^{-1}, prepared by dissolution of ct-DNA in ABS solution, pH 3. Stock solution of Zr(IV) was prepared by dissolution of a required amount of $ZrCl_4$ in 0.1 M HNO_3. The glassware was soaked in 6 M HNO_3 and carefully cleaned before use to avoid contamination. The test solutions were deaerated with high purity argon gas for 10 min before each experiment, and blanketed with the gas during the experiments.

2.2. Instrumentation

Electrochemical measurements were performed on Potentiostat/Galvanostat Autolab30 or EG&G273A in a conventional three-electrode glass cell containing modified gold disk as working electrode, a Pt plate (99.99%, 5 cm^2) as auxiliary electrode, and a Ag/AgCl (3 M KCl) as reference electrode. All reported potentials in this work are referenced to the Ag/AgCl electrode. For the EIS studies, a 5 mV ac amplitude potential superimposed on the formal potential of the redox probe ($E^{0'} = +0.20$ V) was applied, and a wide frequency range from 10 kHz to 100 mHz was scanned. All experiments were performed at room temperature.

2.3. Preparation of Au–MPA SAM electrode

The gold disk electrode (Azar electrode, Urmia, I.R. IRAN, 0.0942 cm^2) was polished using aqueous slurries of alumina (0.30 down to 0.05 μm), sonicated in water/chloroform/water for 5 min, and then cleaned electrochemically by cycling the electrode potential between 0.00 and +1.50 V terminated at 0.00 V vs. Ag/AgCl in 0.5 M sulfuric acid, until reproducible voltammograms were observed [31]. A roughness factor of 1.92 ± 0.12 was calculated from the ratio of real to geometric surface area, and attempted to maintain it constant in all experiments [32]. The real surface area was calculated by integration of the cathodic peak observed during redox reaction of gold, assuming 482 μC cm^{-2} charge for reduction of one monolayer of AuO on Au (111) [33]. Before modification, the electrode was thoroughly rinsed with ethanol and water. The cleaned Au electrode was modified by sonicating in a 2.0×10^{-2} M MPA aqueous solution for 15 min, and then, keeping in this solution for six more hours to form Au–MPA SAM electrode.

2.4. Preparation of Au–MPA–Zr(IV) SAM electrode

Immobilization of Zr(IV) was carried out under open-circuit potential by immersion of the Au–MPA SAM electrode into a 10 ml stirring solution of 1.0×10^{-3} M Zr(IV) at pH ~ 1 to form Au–MPA–Zr (IV) electrode. Our preliminary studies showed that almost after 15 min incubation, the surface was saturated with Zr(IV), and higher incubation times did not change the results significantly. The modified electrode was removed, rinsed with 0.1 M HNO_3, and used immediately for immobilization of ct-DNA.

2.5. Determination of ct-DNA

Initial studies on the adsorption of ct-DNA was performed by immersion of Au–MPA–Zr(IV) electrode in a 1.0×10^{-6} g mL^{-1} ct-DNA solution with different pHs at the open-circuit potential for about 5 min, while the solution was gently stirred. Accumulation (a) and quantitative determination (b) of DNA were performed under tested conditions as: (a) 5 min incubation in acetate buffer saline (ABS) solution, pH 3, containing different concentration of DNA, and (b) electrochemical determination in the presence of 5.0×10^{-4} M $[Fe(CN)_6]^{3-}$ in ABS at pH 3 using CV, OSWV, and EIS techniques.

3. Results and discussion

3.1. Preparation and characterization of Au–MPA–Zr(IV) SAM electrode

Preparation of Au–MPA–Zr(IV) in context with the chemistry of Zr (IV) in aqueous solution [34,35], stability of Zr(IV) at very acidic pHs [36,37], and immobilization of Zr(IV) on Au–MPA SAM electrode from an aqueous solution was reported in our previous work [30]. The main purpose of the present work was to use immobilized Zr(IV) as a glue for accumulation, and then, electrochemical determination of ct-DNA on the modified electrode in the presence of $[Fe(CN)_6]^{3-}$ redox probe.

Preparation and characterization of the Au–MPA–Zr(IV) SAM will be discussed briefly first, then, we will concentrate on the quantitative determination of ct-DNA. Layer-by-layer modifications of the surface, formation of Au–MPA–Zr(IV) SAM and its interaction with DNA, were monitored by CV. Cyclic voltammograms obtained at pH 3 on Au electrode before and after each step of modification are presented in Fig. 1. Formation of MPA SAM on Au electrode decreased the faradaic peak currents (i_ps), and increased the peak separation (ΔE_p) (Fig. 1,

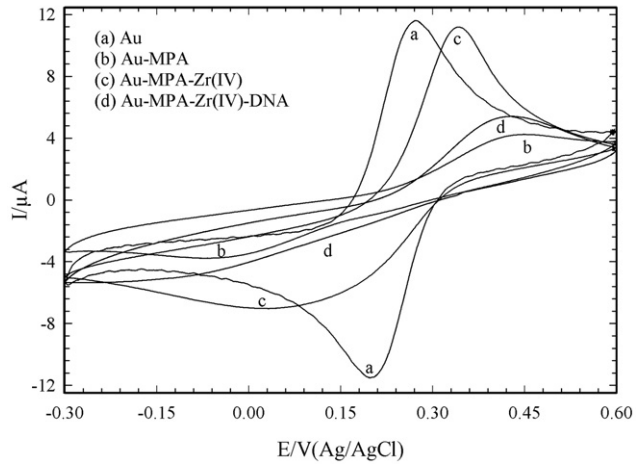

Fig. 1. Cyclic voltammograms obtained in the presence of 5.0×10^{-4} M $[Fe(CN)_6]^{3-}$ as a redox probe, in ABS solution at pH 3, containing 1.0×10^{-2} M NaCl as a supporting electrolyte, on Au electrode before and after each step of modification; (a) bare Au, (b) Au–MPA, (c) Au–MPA–Zr(IV), and (d) Au–MPA–Zr(IV)–DNA. Scan rate is 100 mV s^{-1}.

compare curves a and b). These observations are in agreement with those previously reported on Au–MPA SAM [30]. However, after incubation of Au–MPA SAM electrode in acidic solution of Zr(IV), the i_ps were increased and ΔE_p were decreased (Fig. 1 curve c). The reason of this behavior is described as follows: pH-metric titration curves obtained using variation of the i_ps and ΔE_p of Au–MPA–Zr(IV) electrode as a function of pH revealed a surface pK_a of 5.5, and thus, a positive charge-state of the surface at lower pH values (Fig. 2). Therefore, it can be assumed that the increases in i_ps as well as the decreases in ΔE_p, observed on Au–MPA–Zr(IV) SAM, have been originated from electrostatic attraction between positively charged surface of Au–MPA–Zr(IV) SAM electrode at acidic solutions and $[Fe(CN)_6]^{3-}$ redox probe.

3.2. Interaction of Au–MPA–Zr(IV) electrode with ct-DNA

Interaction of immobilized Zr(IV) with phosphate and carboxylic groups has been investigated [23,38], specially, as a glue between pectin carboxylate and DNA phosphate groups for analytical purposes [39]. We expect that ionic adsorption of ct-DNA by immobilized Zr(IV)

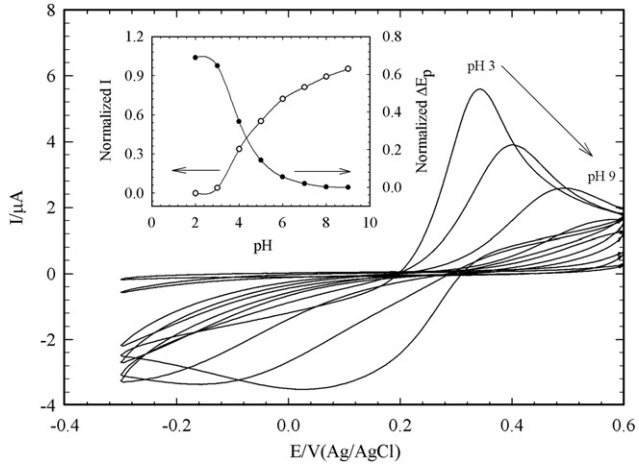

Fig. 2. Cyclic voltammograms obtained on Au–MPA–Zr(IV) SAM electrodes in the presence of 5.0×10^{-4} M $[Fe(CN)_6]^{3-}$ in ABS containing 1.0×10^{-2} M NaCl; scan rate is 100 mV s^{-1}. Outer to inner; pH 3.0, 4.0, 5.0, 6.0, 7.0, 8.0 and 9.0. Inset shows variation of normalized i_p and ΔE_p extracted from cyclic voltammograms of Au–MPA–Zr(IV) SAM electrodes, normalized i_p and ΔE_p are $(i_p(max)-i_p)/i_p(max)$ and $(\Delta E_p(max)-\Delta E_p)/\Delta E_p(max)$, respectively. It was difficult to find E_p at alkaline pHs, thus, $\Delta E_p(max)$ was equaled to the potential window in normalization process.

on the topside of Au–MPA SAM (recognition system) can block the charge transfer between reversible redox reaction of a probe and metallic base of the gold modified electrode, and thus, affect on electrochemical signals (transducers), e.g. i_p and R_{ct}, leading to a new electrochemical method for ct-DNA determination.

Cyclic voltammograms obtained on Au–MPA–Zr(IV) electrode at pH 3, before and after 5 min incubation in 1.0×10^{-6} g mL^{-1} ct-DNA solution, are presented in Fig. 1. Adsorption of ct-DNA on Au–MPA–Zr(IV) electrode has decreased the i_ps and increased ΔE_ps (Fig. 1, compare curves c and d). This effect can be explained as follow; (i) Adsorption of ct-DNA has changed the charge state of the electrode surface to negative, so, the negatively charged redox probe $[FeCN_6]^{3-}$ has been repelled from the electrode surface. (ii) On the other hand, phosphodiester backbone of ct-DNA is supposed to be bridged between the immobilized Zr(IV). Therefore, the electrode surface has been strongly blocked and the charge transfer kinetic has been decreased.

The mechanism of the electrode blocking either by electrostatics or by phosphodiester backbone bridging by Zr(IV) should be easily resolved by using positively charged $[Ru(NH_3)_6]^{3+/2+}$ probe. We verified this object by the EIS (Fig. 3) and CV measurements in the presence of $[Ru(NH_3)_6]^{3+/2+}$ during layer-by-layer assembly process. Kinetic of the electron transfer for $[Ru(NH_3)_6]^{3+/2+}$ is very fast [40], specially on the short chain thiol (MPA) that was used in this work. Thus, we expected almost no isolation effect. This expectation was practically supported by these results, compare curves a and b with curve c. After accumulation of Zr(IV) on the surface of Au–MPA, isolation effects were obviously observed due to both electrostatic repulsion and blocking effect of Zr(IV), compare curves a and b with curve c.

Finally, accumulation of DNA on the surface of Au–MPA–Zr(IV) blocked effectively the surface (Fig. 3, curve (d)). This behavior is resultant of two effects; (i) electrostatic attraction between positively charged probe $[Ru(NH_3)_6]^{3+}$ and negatively charged surface, Au–MPA–Zr(IV)–DNA that decreases the R_{ct}. (ii) Blocking of the redox reaction of $[Ru(NH_3)_6]^{3+}$ by *bridging of phosphodiester backbone of DNA on Zr(IV)* that increases the R_{ct}. The observed behavior is resultant of these two effects with dominant effect of bridging of *phosphodiester backbone of DNA* (i.e. increasing of R_{ct}). See Fig. 3, curve d. Similar tendency, but with lower sensitivity, was observed by CV measurements (data not shown).

High concentrations of the electrolytes (salts) effectively inhibit DNA electrostatic interaction bindings [41]. So, it was necessary to investigate effect of ionic strength of the incubation solution on the

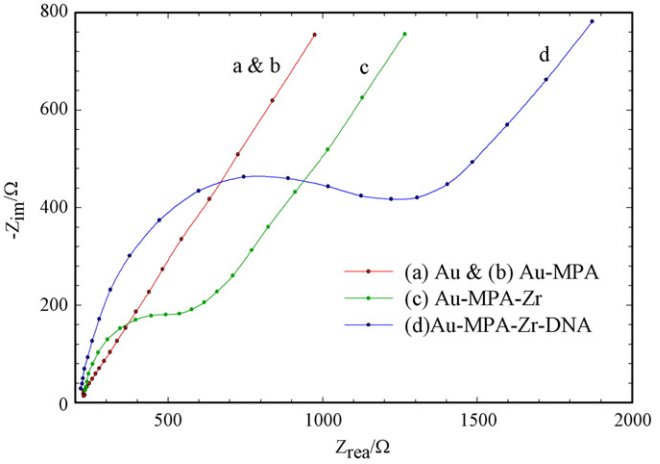

Fig. 3. Complex plane plots of the EIS obtained in the presence of 0.5 mM $[Ru(NH_3)_6]^{3+/2+}$ as a positively charged redox probe, in ABS solution at pH 3, containing 1.0×10^{-2} M NaCl as a supporting electrolyte, on Au electrode during layer-by-layer assembly process; (a) bare Au, (b) Au–MPA, (c) Au–MPA–Zr(IV), and (d) Au–MPA–Zr(IV)–DNA. $E_{dc}=-0.1$ V vs. Ag/AgCl, $E_{ac}=+5$ mV, frequency range from 10 MHz to 0.1 Hz.

amount of ct-DNA adsorbed on Au–MPA–Zr(IV) electrode. For concentrations higher than 2.0×10^{-2} M NaCl, the results were not reproducible and the sensitivity was low. Two reasons might be responsible for this phenomenon; (i) shielding effect of salt ions on phosphate groups of DNA that result in depletion of electrostatic attraction to Zr(IV) [42] and (ii) the coordination of chloride ions with Zr(IV) on the topside of SAM, and thus weakening or breaking the interaction between Zr(IV) and DNA molecules. The best results were obtained in 1.0×10^{-2} M NaCl (data not shown).

Double helix DNA is stable in the pH range of 3.0–10.0 at room temperature according to [43]. However, we also studied the effect of pH on the amount of loaded ct-DNA on Au–MPA–Zr(IV) electrode. For the pHs higher than 5.5, the electrode surface was dramatically blocked by OH groups, and a large decrease in peak currents of $[Fe(CN)_6]^{3-}$ was observed. So, further adsorption of ct-DNA on the electrode surface could not be detected accurately at the pHs higher than 5.5. Indeed, in these conditions, the electrode surface was not favorable for ionic coordination of ct-DNA. These observations could be directly related to the weak adsorption process occurring between phosphodiester groups of ct-DNA and immobilized Zr(IV) at the pHs higher than 5.5. The adsorption of DNA increased by decreasing the pH down to pH 3. Strong interaction between ct-DNA and immobilized Zr (IV) at pH 3 could be reasonably attributed to electrostatic attraction of highly negatively charged ct-DNA (the pK_a of the phosphodiester group is around one [44]) and the positively charged immobilized Zr (IV), and thus, formation of ionic coordination bonds. Due to native ct-DNA structure alteration [45], no experiment was performed at pHs lower than 3.

As a conclusion, a good affinity was observed for Zr(IV) towards the Au–MPA, and for phosphate backbone of ct-DNA towards the Au–MPA–Zr(IV) SAM electrodes at the tested experimental conditions. This behavior was used as a base in the present work to develop a new method for quantitative determination of ct-DNA.

3.3. Analytical performance of Au–MPA–Zr(IV) electrode for ct-DNA determination

(i) Cyclic voltammograms obtained on Au–MPA–Zr(IV) electrode in ABS solution at pH 3 in the presence of $[FeCN_6]^{3-}$ redox probe, after accumulation of ct-DNA are presented in Fig. 4. A linear calibration curve with three orders of magnitude in logarithmic scale, and R.S.Ds varied from 3.0 to 5.14% for $n=4$ at each point, in the range of 5.0×10^{-8} to 1.0×10^{-5} g mL^{-1}

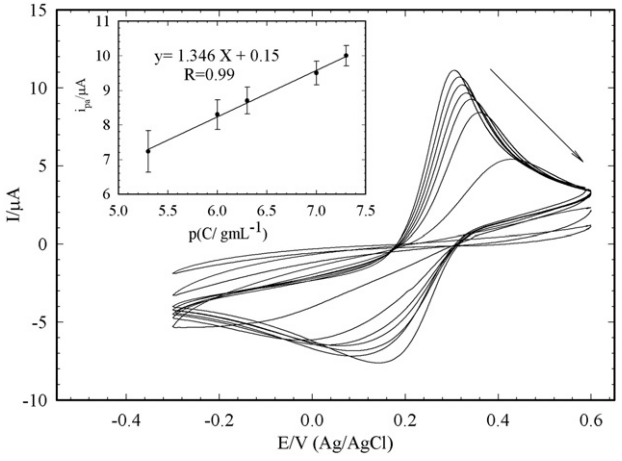

Fig. 4. Cyclic voltammograms obtained of 5.0×10^{-4} M $[Fe(CN)_6]^{3-}$ redox probe on Au–MPA–Zr(IV) electrode in ABS containing 1.0×10^{-2} M NaCl at pH 3, after 5 min accumulation of DNA at pH 3 from solutions containing different concentrations of calf thymus DNA. Scan rate is 100 mV s^{-1}. The calibration curve extracted from variations of i_{pa}s as function of ct-DNA concentration from 5.0×10^{-8} to 5.0×10^{-5} g mL^{-1}. $I_{p,a}/\mu A = 1.346\ p[C_{DNA}/(g\ mL^{-1})]/\mu A + 0.15/\mu A$, $R=0.99$.

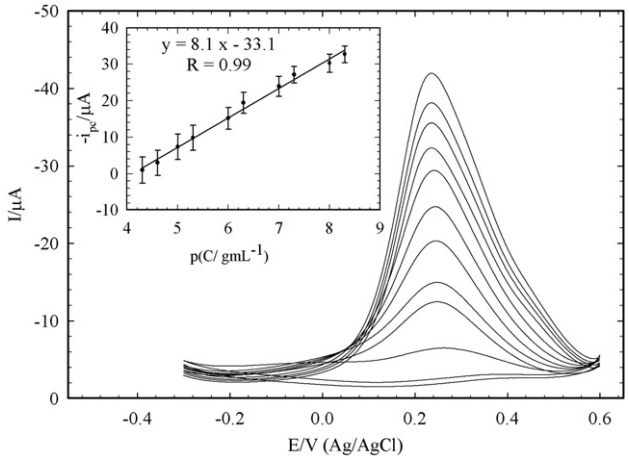

Fig. 5. Osteryoung square wave voltammograms of $[Fe(CN)_6]^{3-}$ redox probe on Au–MPA–Zr(IV) electrode obtained at frequency of 25 Hz and scan rate of 22.5 mV s^{-1} after accumulation of DNA from solutions containing different concentrations of ct-DNA. Other conditions were the same as those cited in Fig. 4. The calibration curves obtained from variations of $-i_{pc}$s as function of ct-DNA concentration from 5.0×10^{-9} to 5.0×10^{-5} g mL^{-1}. $I_{p,c}/\mu A = 8.10\ p[C_{DNA}/(g\ mL^{-1})]/\mu A + 33.10/\mu A$, $R=0.99$.

DNA was observed using anodic peak currents as a function of ct-DNA concentration in accumulation solutions (Fig. 4, inset), $\{I_{p,a}/\mu A = 1.346\ p[C_{DNA}/(g\ mL^{-1})]/\mu A + 0.15/\mu A,\ R=0.99\}$.
The results indicated that the Au–MPA–Zr(IV) SAM electrode was an appropriate sensor for detection of ct-DNA. However, due to inherent disadvantages, like small sensitivity, and large and uncertain contribution of background currents (high detection limit), accompanying the CV method [46], the merits obtained in this part did not satisfy our requirements for quantitative chemical analysis; i.e. low detection limit, and high sensitivity and accuracy. On the other hand, extraction of peak currents was difficult and insignificant at concentrations above 1.0×10^{-5} g mL^{-1} of ct-DNA, i.e., the CVs became flat and merged each other. Consequently, OSWV that benefits of high sensitivity and low detection limit (small contribution of background in analytical signal) was employed.

(ii) OSWVs obtained in the abovementioned conditions are presented in Fig. 5. A linear calibration curve, with four orders of magnitude in logarithmic scale, and lower R.S.Ds (in comparison with CV, Fig. 4) varied from 2.3 to 3.6% for $n=4$ at each point, was found (Fig. 5, inset) in the range of 5.0×10^{-9} to 5.0×10^{-5} g mL^{-1} ct-DNA using cathodic peak currents as a function of ct-DNA concentration in accumulation solutions $\{I_{p,c}/\mu A = 8.10\ p[C_{DNA}/(g\ mL^{-1})]/\mu A + 33.10/\mu A,\ R=0.99\}$. Although the OSWV method overcomes several of the limitations accompanying the CV method, it still includes running potentials far from equilibrium, which is possibly undesirable [47].

(ii) EIS is a powerful, non-destructive, and informative technique to examine the microscopic interfacial events (such as complexation and precipitation) or diffusion effects at the modified electrodes near or far from the equilibrium potentials, and serve as a transducer [48–50]. In order to obtain more *precise* and *accurate* data for quantitative determination of ct-DNA, the EIS measurements were performed in the conditions tested for OSWV measurements, but at a constant DC potential of +0.20 V vs. Ag/AgCl reference electrode. The EIS complex plane plots recorded on Au–MPA–Zr(IV) modified electrode as a function of ct-DNA concentration in accumulation solution are presented in Fig. 6. A wide linear dynamic range calibration curve from 5.0×10^{-7} to 1.0×10^{-4} g mL^{-1} DNA as $\{R_{ct}/k\Omega = 9.90\ [C_{(DNA}/g\ mL^{-1})\times10^{-6}]/k\Omega + 30.10/k\Omega\}$ with R.S.Ds varied from 1.8 to 3.2% for $n=4$ at each point and a detection limit of 9.5×10^{-8} g mL^{-1} was obtained. The

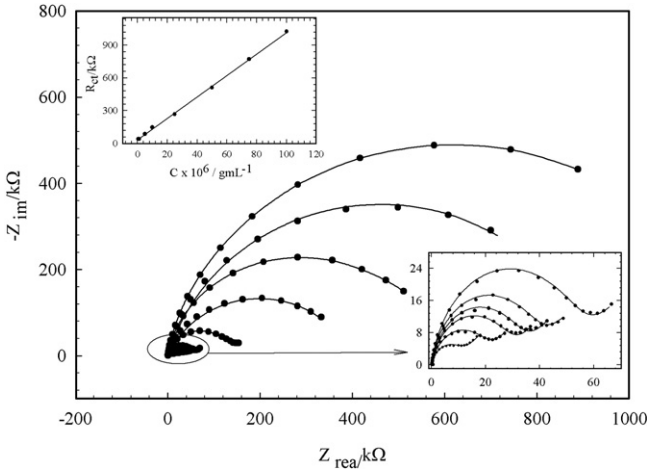

Fig. 6. The EIS complex plane plots obtained for determination of ct-DNA in the presence of 5.0×10^{-4} M $[Fe(CN)_6]^{3-}$ redox probe on Au–MPA–Zr(IV) electrode in ABS solution containing 1.0×10^{-2} M NaCl at pH 3, after 5 min accumulation of ct-DNA at pH 3 from solutions containing different concentrations of calf thymus DNA. $E_{ac}=5$ mV, $E_{dc}=+0.2$ V vs. Ag/AgCl reference electrode. Inset shows linear variations of the R_{ct} as a function of ct-DNA concentration from 1.0×10^{-7} to 1.0×10^{-4} g mL^{-1}. $R_{ct}/k\Omega=9.90$ $[C_{(DNA}/g\ mL^{-1})\times10^{-6}]/k\Omega+30.10/k\Omega$.

applied DC potential in EIS measurements was quite close to the equilibrium potential. It means that (i) the partial change in the $[Fe(CN)_6]^{3-}$ probe concentration during data acquisition in the EIS measurements has been less than that of OSWV experiments, and (ii) the risk of ZrO_2 formation [47] and deterioration of modified layer has been notably decreased [51].

A comparison may be made between the changes observed in the electrochemical signals during determination of ct-DNA here with those observed previously during determination of phosphate [30]. In the case of ct-DNA in this work, the calibration curve is *non-logarithmic* with a relatively *wide linear range* and only *one slope*, in contrary to those observed for phosphate. These behaviors may be explained briefly as follows:

(i) In the case of phosphate, as a small and simple inorganic molecule, *two* linear range calibration curves were observed in *logarithmic scale* that were explained as following [30]: for lower concentrations of phosphate, accumulation is performed mainly via 1:1:1 for MPA:Zr(IV):PO_4^{3-}. Still, for higher concentrations, the chance for bridging of one PO_4^{3-} between two adjacent immobilized Zr(IV) increases. This effect increases the R_{ct}, and thus, the sensitivity of the electrode more effectively than case 1:1:1. Accordingly, two slopes have been observed. The ct-DNA is a large and complicated biomolecule in comparison with phosphate, and contains phosphodiester chains with a large number of connected phosphate groups, so, unlike the phosphate, even at the low concentrations, bridging of ct-DNA between adjacent immobilized Zr(IV)s is possible. This behavior can block the surface more efficiently (ΔR_{ct} is more than 1×10^3 $k\Omega$, see Fig. 6 in comparison with ~350 $k\Omega$ for phosphate [30]), therefore, the observed sensitivity for ct-DNA is *larger*, and, the extracted calibration curve is *non-logarithmic*.

(ii) Probably some of the laying ct-DNAs have been gotten into an upright position by increasing the concentration that increase the distance between redox probe and the electrode surface. Although, this behavior can decrease the blocking effects partially, but, the total negative charge on the surface and from which, electrostatic repulsions between probe and surface can be increased. The resultant of these effects has affected on R_{ct} and one slope has been observed, i.e. sensitivity has not been changed during ct-DNA additions.

3.4. Interferences

Effect of some co-existing anions, cations, and compounds, on the response of Au–MPA–Zr(IV) SAM for DNA was investigated by EIS. The interfering effect is defined as the concentration of interfering species that can change the electrode response toward the analyte by more than 3δ, where δ is standard deviation of the replicate analyte measured signal. The results showed that the R_{ct} for 1.0×10^{-6} g mL^{-1} ct-DNA was not affected significantly by 100-fold cations Na^+, K^+, Fe^{2+}, Ca^{2+}; physiological compounds like dopamine, ascorbic acid, and uric acid; and anions such as Cl^-, NO_3^-, NO_2^-, $-COO^-$, and ClO_4^-; 50-fold SO_4^{2-}; and 10-fold citrate. Proteins and enzymes like laccase and glucose oxidase interfered significantly. However, the Au–MPA–Zr system could be easily adopted as a detector for chromatographic analysis.

3.5. Reusability and stability of the sensor

Regeneration is one of the most important aspects that should be considered in fabrication of the sensors. The procedure for regeneration of the electrode surface was similar to that previously explained in phosphate determination [30]. Briefly, the ct-DNA coordinated to Zr (IV) was removed (surface recovery) by dipping of the Au–MPA–Zr (IV)–ct-DNA SAM electrode into a 0.1 M KOH solution and keeping under sonication for a 5 min. Then, the Au–MPA–Zr(IV) SAM electrode was removed, washed, and immersed in 0.1 M HNO_3 solution containing 1.0×10^{-3} M Zr(IV) for 1 min to repair the Zr(IV) vacancy places (surface repairing), and finally the electrode was reused. By using this recovery/repairing method, the sensor showed a highly repeatable response. Therefore, the R_{ct} obtained by EIS measurements showed a R.S.D mean values of 1.5% for $n=4$ at 1.0×10^{-6} g mL^{-1} of ct-DNA. The process revealed that ct-DNA could be reversibly adsorbed onto the electrode surface in appropriate conditions.

Au–MPA–Zr(IV) SAM modified electrodes were stored in 1.0×10^{-3} M Zr(IV) at pH ~ 1 under argon atmosphere when they were not in use. The long-term storage stability of the electrode was tested by monitoring the amount of decreases in cathodic peak current of $[Fe(CN)_6]^{3-}$ measured by OSWV after several times storage of modified electrode. A decrease of 4% was observed after about one week, implying good electrode stability.

4. Conclusion

A new sensor was developed for the determination of ct-DNA based on Zr(IV) ion immobilized on gold–mercaptopropionic acid self-assembled monolayer electrode (recognition system) and CV, OSWV, and EIS (transducers) in the presence of $[Fe(CN)_6]^{3-}$ as a redox probe. A linear range calibration curve with a detection limit of 9.5×10^{-8} g mL^{-1} and a mean of R.S.D 2.5% was observed in the best conditions by EIS. The surface was successfully regenerated by sonication in 0.1 M KOH solution; and then, repaired by incubation in 1.0×10^{-3} MZr(IV) with a good reproducibility, the R.S.D was 1.5% for $n=4$ by EIS as the best method in this work.

Acknowledgment

The authors gratefully acknowledge the University of Isfahan providing the facilities for this work.

References

[1] H. Wang, W.R. Li, Y. Lu, N.N. Fu, H.S. Zhang, Spectrophotometric determination of DNA using a near infrared probe 1,1′-disulfobutyl-3,3,3′,3′-tetramethylindotricarbocyanine, Spectrochim. Acta 61 (2005) 2103–2107.

[2] S. Zhang, H. Zhong, C. Ding, Ultrasensitive flow injection chemiluminescence detection of DNA hybridization using signal DNA probe modified with Au and CuS nanoparticles, Anal. Chem. 80 (2008) 7206–7212.
[3] Q.C. Zou, Q.J. Yan, G.W. Song, S.L. Zhang, L.M. Wu, Detection of DNA using cationic polyhedral oligomeric silsesquioxane nanoparticles as the probe by resonance light scattering technique, Biosens. Bioelectron. 22 (2007) 1461–1465.
[4] S. Niu, G. Singh, R.F. Saraf, Label-less fluorescence-based method to detect hybridization with applications to DNA micro-array, Biosens. Bioelectron. 23 (2007) 714–720.
[5] M.R. Fernandez, M.J.V. Gonzalez, M.E.D. Garcia, Room-temperature phosphorescent palladium-porphine probe for DNA determination, Anal. Chem. 69 (1997) 2406–2410.
[6] M.I. Churchwell, F.A. Beland, D.R. Doerge, Quantification of multiple DNA adducts formed through oxidative stress using liquid chromatography and electrospray tandem mass spectrometry, Chem. Res. Toxicol. 15 (2002) 1295–1301.
[7] S. Hason, H. Pivonkova, V. Vetter, M. Fojta, Label-free sequence-specific DNA sensing using copper-enhanced anodic stripping of purine bases at boron-doped diamond electrodes, Anal. Chem. 80 (2008) 2391–2399.
[8] J.M. Pingarron, P.Y. Sedeno, A.G. Cortes, Gold nanoparticle-based electrochemical biosensors, Electrochim. Acta 53 (2008) 5848–5866.
[9] K.A. Howell, E.P. Achterberg, C.B. Braungardt, A.D. Tappin, P.J. Worsfold, D.R. Turner, Voltammetric in situ measurements of trace metals in coastal waters, TrAC 22 (2003) 828–835.
[10] E. Palecek, Oscillographic polarograhpy of nucleic acids and their building blocks, Naturwiss 45 (1958) 186–187.
[11] J. Wang, X. Cai, J. Wang, C. Jonsson, Trace measurements of RNA by potentiometric stripping analysis at carbon paste electrodes, Anal. Chem. 67 (1995) 4065–4070.
[12] C. Fan, H. Song, X. Hu, G. Li, J. Zhu, X. Xu, D. Zhu, Voltammetric response and determination of DNA with a silver electrode, Anal. Biochem. 271 (1999) 1–7.
[13] W. Sun, Y. Li, Y. Duan, K. Jiao, Direct electrocatalytic oxidation of adenine and guanine on carbon ionic liquid electrode and the simultaneous determination, Biosens. Bioelectron. 24 (2008) 994–999.
[14] M.E. Napier, D.O. Hull, H.H. Thorp, Electrocatalytic oxidation of DNA-wrapped carbon nanotubes, J. Am. Chem. Soc. 127 (2005) 11952–11953.
[15] M.R. Gore, V.A. Szalai, P.A. Ropp, I.V. Yang, J.S. Silverman, H.H. Thorp, Detection of attomole quantitites of DNA targets on gold microelectrodes by electrocatalytic nucleobase oxidation, Anal. Chem. 75 (2003) 6586–6592.
[16] F. Mizutani, S. Yabuki, Y. Sato, S. Iijima, Amperometric measurement of ds-DNA content using a peroxidase-modified electrode, Bioelectrochemistry 63 (2004) 257–259.
[17] R.K. Shervedani, F. Yaghoobi, A.H. Mehrjardi, S.M.S. Barzoki, Electrocatalytic activities of gold-5-amino-2-mercaptobenzimidazole-M^{n+} self-assembled monolayer complexes (M^{n+}:Ag^{+}, Cu^{2+}) for hydroquinone oxidation investigated by CV and EIS, Electrochim. Acta 53 (2008) 4185–4192.
[18] R.K. Shervedani, S.A. Mozaffari, Copper(II) nanosensor based on a gold cysteamine self-assembled monolayer functionalized with salicylaldehyde, Anal. Chem. 78 (2006) 4957–4963.
[19] R.K. Shervedani, A.H.H. Mehrjardi, N. Zamiri, Bioelectrochemistry 69 (2006) 201–208.
[20] R.K. Shervedani, A.H.H. Mehrjardi, Comparative electrochemical behavior of glucose oxidase covalently immobilized on mono-, di- and tetra-carboxylic acid functional Au–thiol SAMs via anhydride–derivatization route, Sens. Actuators B 137 (2009) 195–204.
[21] R.K. Shervedani, M. Bagherzadeh, Hydroxamation of gold surface via in-situ layer-by-layer functionalization of cysteamine self-assembled monolayer: preparation and electrochemical characterization, Electrochim. Acta 53 (2008) 6293–6303 and references there in.
[22] H. Lee, L.J. Kepley, H.G. Hong, S. Akhter, T.E. Mallouk, Adsorption of ordered zirconium phosphonate multilayer films on silicon and gold surfaces, J. Phys. Chem. 92 (1988) 2597–2601.
[23] M. Fang, D.M. Kaschak, A.C. Sutorik, T.E. Mallouk, A "mix and match" ionic–covalent strategy for self-assembly of inorganic multilayer films, J. Am. Chem. Soc. 119 (1997) 12184–12191.
[24] S.B. Bakiamoh, G.J. Blanchard, Demonstration of oriented multilayers through asymmetric metal coordination chemistry, Langmuir 15 (1999) 6379–6385.
[25] M. Mazur, P. Krysinski, G.J. Blanchard, Use of zirconium–phosphate–carbonate chemistry to immobilize polycyclic aromatic hydrocarbons on boron-doped diamond, Langmuir 21 (2005) 8802–8808.
[26] M. Mazur, P. Krysiński, A.M. Kamińska, J. Bukowska, J. Rogalski, G.J. Blanchard, Immobilization of laccase on gold, silver and indium tin oxide by zirconium–phosphonate–carboxylate (ZPC) coordination chemistry, Bioelectrochemistry 71 (2007) 15–22.
[27] J. Wang, F. Wang, Z. Xu, Y. Wang, S. Dong, Surface plasmon resonance and electrochemistry characterization of layer-by-layer self-assembled DNA and Zr^{4+} thin films, and their interaction with cytochrome c, Talanta 74 (2007) 104–109.
[28] S.Q. Liu, J.J. Xu, H.Y. Chen, A reversible adsorption–desorption interface of DNA based on nano-sized zirconia and its application, Colloids Surf. B 36 (2004) 155–159.
[29] J. Monot, M. Petit, S.M. Lane, I. Guisle, J. Léger, C. Tellier, D.R. Talham, B. Bujoli, Towards zirconium phosphonate-based microarrays for probing DNA–protein interactions: critical influence of the location of the probe anchoring groups, J. Am. Chem. Soc. 130 (2008) 6243–6251.
[30] R.K. Shervadani, S. Pourbeyram, Zirconium immobilized on gold–mercaptopropionic-acid self-assembled monolayer for trace determination of phosphate in blood serum by using CV, EIS, and OSWV, Biosens. Bioelectron. 24 (2009) 2199–2204.
[31] J.P. Hoare, A cyclic voltammetric study of the gold–oxygen system, J. Electrochem. Soc. 131 (1984) 1808–1815.
[32] S.E. Creager, L.A. Hockett, G.K. Rowe, Consequences of microscopic surface roughness for molecular self-assembly, Langmuir 8 (1992) 854–861.
[33] U. Oesch, J. Janata, Electrochemical study of gold electrodes with anodic oxide films-I. Formation and reduction behavior of anodic oxides on gold, Electrochim. Acta 28 (1983) 1237–1246.
[34] A. Singhal, L.M. Toth, J.S. Lin, K. Affholter, Zirconium(IV) tetramer/octamer hydrolysis equilibrium in aqueous hydrochloric acid solution, J. Am. Chem. Soc. 118 (1996) 11529–11534.
[35] M.B. Gholivand, A. Babakhanian, M. Joshaghani, Zirconium ion selective electrode based on bis(diphenylphosphino) ferrocene incorporated in a poly(vinyl chloride) matrix, Anal. Chim. Acta, 584 (2007) 302–307.
[36] R. Ott, R. Kramer, Rapid phosphodiester hydrolysis by zirconium (IV), Angew. Chem. Int. Ed. 37 (1998) 1957–1960.
[37] D.I. Ryabchikov, I.N. Marov, A.N. Ermakov, V.K. Belyaeva, Stability of some inorganic and organic complex compounds of zirconium and hafnium, J. Inorg. Nucl. Chem. 26 (1964) 965–980.
[38] G.L. Lundquist, J.A. Cox, Surface second harmonic generation from asymmetric multilayer assemblies: gaining insight into layer-dependent order, Langmuir 17 (2001) 3438–3446.
[39] J. Kong, A.R. Ferhan, X. Chen, L. Zhang, N. Balasubramanian, Polysaccharide templated silver nanowire for ultrasensitive electrical detection of nucleic acids, Anal. Chem. 80 (2008) 7213–7217.
[40] V. Ganesh, V. Lakshminarayanan, Scanning tunneling microscopy, Fourier transform infrared spectroscopy, and electrochemical characterization of 2-naphthalenethiol self-assembled monolayers on the Au surface: a study of bridge-mediated electron transfer in $Ru(NH_3)_6^{2+}|Ru(NH_3)_6^{3+}$ redox reactions, J. Phys. Chem. B 109 (2005) 16372–16376.
[41] E.M. Boon, N.M. Jackson, M.D. Wightman, S.O. Kelley, M.G. Hill, J.K. Barton, Intercalative stacking: a critical feature of DNA charge-transport electrochemistry, J. Phys. Chem. B 107 (2003) 11805–11812.
[42] J. Li, C. Bai, C. Wang, C. Zhu, Z. Lin, Q. Li, E. Cao, A convenient method of aligning large DNA molecules on bare mica surfaces for atomic force microscopy, Nucleic Acids Res. 26 (1998) 4785–4786.
[43] M.T. Record Jr., Electrostatic effects on polynucleotide transitions. II. Behavior of titrated systems, Biopolymers 5 (1967) 993–1008.
[44] C.R. Cantor, P.R. Schimmel, Biophysical Chemistry, W.H. Freeman and Company, New York, 2002.
[45] E.L. Duggan, V.L. Stevens, B.W. Grunbaum, Deformation of deoxyribonucleate. I. Titration and optical absorption studies of the effect of temperature, ionic strength and pH on DNA structure, J. Am. Chem. Soc. 79 (1957) 4859–4863.
[46] A.J. Bard, L.R. Faulkner, Electrochemical Methods, Fundamentals and Applications, Wiley, New York, 2001, p. 240.
[47] K. Bandyopadhyay, K. Vijayamohanan, Formation of microcrystalline zirconia using the functionalized interface of a self-assembled monolayer of dithiol on polycrystalline gold at room temperature, Langmuir 14 (1998) 6924–6929.
[48] E. Barsoukov, J.R. Macdonald, Impedance Spectroscopy, Theory, Experiment and Applications (Eds.), Wiley, New York, 2005.
[49] Y. Wang, C. Li, X. Li, Y. Li, H.B. Kraatz, Unlabeled hairpin-DNA probe for the detection of single-nucleotide mismatches by electrochemical impedance spectroscopy, Anal. Chem. 80 (2008) 2255–2260.
[50] C.P. Chen, A. Ganguly, C.H. Wang, C.W. Hsu, S. Chattopadhyay, Y.K. Hsu, Y.C. Chang, K.H. Chen, L.C. Chen, Label-free dual sensing of DNA molecules using GaN nanowires, Anal. Chem. 81 (2009) 36–42.
[51] Z. Tong, R. Yuan, Y. Chai, Y. Xie, S. Chen, A novel and simple biomolecules immobilization method: electro-deposition ZrO_2 doped with HRP for fabrication of hydrogen peroxide biosensor, J. Biotechnol. 128 (2007) 567–575.